


Article

Deciphering the Role of V88L Substitution in NDM-24 Metallo- β -Lactamase

Zhihai Liu ^{1,2} , Alessandra Piccirilli ³, Dejun Liu ², Wan Li ², Yang Wang ² and Jianzhong Shen ^{2,*}¹ Agricultural Bio-pharmaceutical Laboratory, College of Chemistry and Pharmaceutical Sciences, Qingdao Agricultural University, Qingdao 266109, China² Beijing Advanced Innovation Center for Food Nutrition and Human Health, College of Veterinary Medicine, China Agricultural University, Beijing 100193, China³ Dipartimento di Scienze Cliniche Applicate e Biotecnologiche, Università degli Studi dell'Aquila, 67100 L'Aquila, Italy

* Correspondence: sjz@cau.edu.cn; Tel.: +86-10-62732803; Fax: +86-10-62731032

Received: 25 July 2019; Accepted: 28 August 2019; Published: 2 September 2019



Abstract: The New Delhi metallo- β -lactamase-1 (NDM-1) is a typical carbapenemase and plays a crucial role in antibiotic-resistance bacterial infection. Phylogenetic analysis, performed on known NDM-variants, classified NDM enzymes in seven clusters. Three of them include a major number of NDM-variants. In this study, we evaluated the role of the V88L substitution in NDM-24 by kinetical and structural analysis. Functional results showed that V88L did not significantly increase the resistance level in the NDM-24 transformant toward penicillins, cephalosporins, meropenem, and imipenem. Concerning ertapenem, *E. coli* DH5 α /NDM-24 showed a MIC value 4-fold higher than that of *E. coli* DH5 α /NDM-1. The determination of the k_{cat} , K_m , and k_{cat}/K_m values for NDM-24, compared with NDM-1 and NDM-5, demonstrated an increase of the substrate hydrolysis compared to all the β -lactams tested, except penicillins. The thermostability testing revealed that V88L generated a destabilized effect on NDM-24. The V88L substitution occurred in the β -strand and low β -sheet content in the secondary structure, as evidenced by the CD analysis data. In conclusion, the V88L substitution increases the enzyme activity and decreases the protein stability. This study characterizes the role of the V88L substitution in NDM-24 and provides insight about the NDM variants evolution.

Keywords: New Delhi metallo- β -lactamase; NDM-24; kinetic profile; secondary structure

1. Introduction

Metallo- β -lactamases (MBLs) are a group of enzymes that confer high resistance to most β -lactams. The active site of these enzymes contains one or two zinc ions, that are crucial for catalytic mechanism [1]. Based on their amino acid sequences, MBLs have been divided into subclasses B1, B2, and B3 [2]. Among subclass B1, the New Delhi metallo- β -lactamase (NDM-1) is one of the most widespread carbapenemase. NDM-1 was first identified in 2008 in a clinical strain of *Klebsiella pneumoniae* [3]. NDM-1 producing bacteria can hydrolyse all β -lactams (except monobactams), including carbapenems, the “last resort” antibiotics used in clinical therapy. NDM-1 genes are located on plasmids that mediate their dissemination across different bacterial strains [4,5]. However, the clinical success of NDM is also due to the fact that it is a lipoprotein anchored to the outer membrane, resulting in an unusual stability of NDM-1 and enabling secretion, in Gram-negative bacteria [6–8].

To date, more than 26 variants differing by a limited number of substitutions have been identified [9]. Previous studies revealed that these substitutions have contributed to NDM-1 to increase the hydrolytic activity toward several β -lactams resulting in an increment of resistance in the host bacteria [10]. Crystal structures showed that NDM-1 presents the typical $\alpha\beta/\beta\alpha$ fold of MBLs [11,12]. In this

enzyme, the zinc ions are coordinated by six conserved residues: H120, H122, and H189 for Zn1 (BBL numbering) and D124, C208, and H250 for Zn2 (BBL numbering). The active site is surrounded by Loop 3 (residues 67-73) and Loop 10 (residues 210-230), involved in the substrate accommodation [12]. The most frequent substitution in NDM-1 is M154L, found in 11 NDM variants (NDM-4, -5, -7, -8, -12, -13, -15, -17, -19, -20 and -21) [9,13–16]. Indeed, V88L has been reported in five NDM variants (NDM-5, -17, -20, -21 and -24). Other frequent substitutions are A233V (NDM-6, -15, -19 and -27), D130G (NDM-8 and -14), D130N (NDM-7 and -19), and D95N (NDM-3 and -27) [10]. The single substitutions of M154L and D130G seem to increase the carbapenemase activity in NDM-4 and NDM-14, respectively [17,18]. Moreover, the combination D130G/M154L (NDM-8), reduces the hydrolysis toward carbapenems [19]. The main goal of the study was to evaluate the role of the V88L substitution in the NDM-24 enzyme. The NDM-24 was generated in the laboratory by a site-directed mutagenesis of NDM-1 and the enzyme properties, protein structure, and thermal stability were studied compared with NDM-1 and NDM-5.

2. Results and Discussion

2.1. Phylogenetic Analysis

A phylogenetic analysis of NDM-1 variants was performed in order to classify these enzymes based on their amino acid similarities. Overall, the NDM variants were classified into three major clusters (NDM-1, NDM-4, and NDM-24), two minor clusters (NDM-3 and NDM-6), and two divergent proteins (NDM-14 and NDM-10). As shown in Figure 1, the NDM variants are well categorized. The NDM-1 cluster includes eight variants that showed only one amino acid replacement, except for NDM-18 where an insertion of five amino acids have been found (position 48-52). In the NDM-4 group, all variants possess the replacement at position 154. In particular, except for NDM-11 containing the M154V substitution, all variants shared M154L. In the NDM-24 group, Valine at position 88 has been replaced by a Leucine (V88L). Concerning the two minor groups, similar characteristics were observed with the D95N and A233V substitution for the NDM-3 and NDM-6 clusters, respectively.

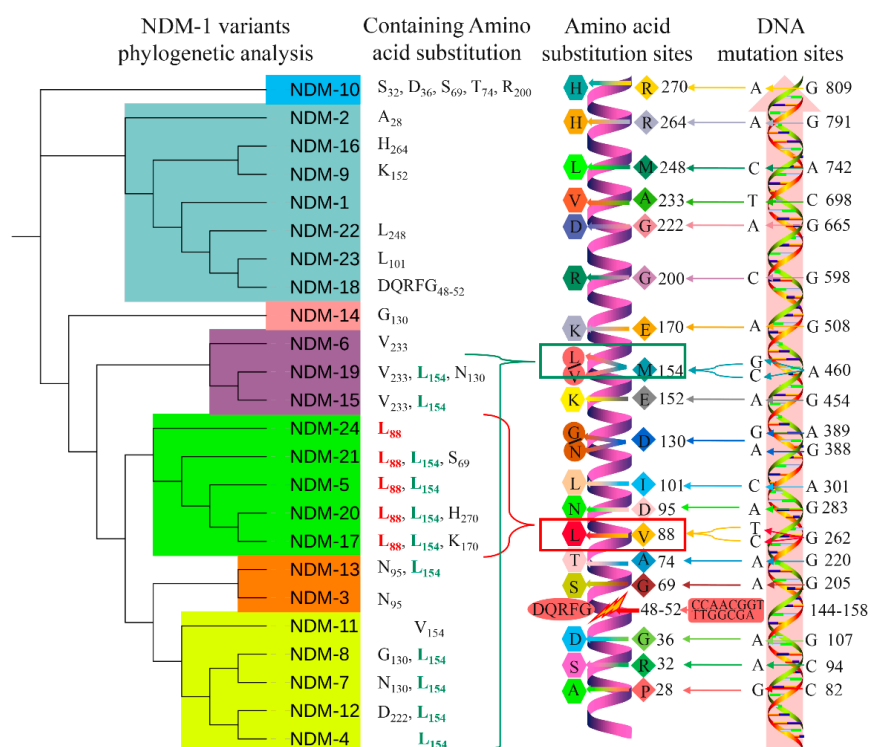


Figure 1. New Delhi metallo-β-lactamase-1 (NDM-1) variants phylogenetic analysis. Phylogenetic groups were differently coloured: For example, the NDM-24 cluster is coloured in green.

2.2. Functional Study

The NDM-24 variant was obtained by a site-directed mutagenesis by using the NDM-1 as template. All genes (bla_{NDM-1} , bla_{NDM-5} , and bla_{NDM-24}) were cloned into pHSG398, which were controlled by the same promoter and thus the same expression. The *E. coli* DH5 α recombinant strains were used to test susceptibility to a wide panel of β -lactams. As shown in Table 1, the results of the susceptibility test revealed that NDM-1, NDM-5, and NDM-24 confer resistance to most β -lactams with similar MIC values, suggesting that the NDM enzymes were successfully expressed in the host cells. A different behaviour was observed for carbapenems, for which the MIC values were markedly lower than those of penicillins and cephalosporins with the exception of ceftapime, as previously reported [15–20]. Concerning ertapenem, NDM-24 and NDM-5 showed an increase of the MIC values of the 4- and 8-fold with respect to NDM-1. Based on the data obtained, the V88L substitution enhances resistance toward ertapenem.

Table 1. Antimicrobial susceptibility of *E. coli* BL21(DE3)-DH5 α carrying bla_{NDM-1} , bla_{NDM-5} , and bla_{NDM-24} .

Antibiotic	MIC (μ g/mL)			
	<i>E. coli</i> DH5 α /pHSG398	<i>E. coli</i> DH5 α /pHSG398 -NDM-24	<i>E. coli</i> DH5 α /pHSG398 -NDM-1	<i>E. coli</i> DH5 α /pHSG398 -NDM-5
Ampicillin	2	>256	>256	>256
Penicillin G	16	>256	>256	>256
Aztreonam	0.031	0.031	0.031	0.031
Cefepime	0.031	2	1	2
Cefotaxime	0.062	32	64	64
Cefoxitin	2	128	128	128
Ceftazidime	0.125	256	256	256
Cefazolin	2	128	128	256
Ertapenem	0.015	1	0.25	2
Imipenem	0.062	2	2	2
Meropenem	0.031	1	1	2

2.3. Characteristics of Enzyme Activity

In order to obtain soluble and active enzymes, the recombinant plasmids were successfully expressed in the *E. coli* BL21 (DE3) cells as described in the methods section. After purification, the enzymes were checked on SDS-PAGE to confirm the solubility and purity (>90%) (Figure S1). The MALDI-TOF mass spectrometry was used to confirm the molecular mass of the three enzymes, which corresponds to 24884,024 Da (Figure S2). To investigate the enzyme activity, the kinetic parameters for NDM-1, NDM-5, and NDM-24 were determined (Table 2).

All the NDM variants of this study were able to hydrolyse all the β -lactams tested. Compared with NDM-1, NDM-24 showed lower K_m values for penicillins and ceftazidime whereas for carbapenems they are quite similar. Comparing the k_{cat} values, NDM-24 hydrolyses all β -lactams, except penicillins, better than NDM-1 and NDM-5. In particular, the k_{cat} values of NDM-24 are 2.26-, 1.61-, 2.73-, 2.02-, 2.17-, and 1.75-fold higher than NDM-1 towards penicillin G, ceftazidime, cefepime, imipenem, meropenem, and ertapenem, respectively. This was also confirmed by a slight increase of catalytic efficiency. This result stated the important role of V88L in the substrate hydrolysis. The contribution of V88L is likely that of M154L as demonstrated by the calculation of the k_{cat}/K_m rates (Table 2). This was possibly due to differences in the intrinsic properties, such as the enzyme stability, protein expression, and adaptability [21–24], and nutritional conditions of bacteria in vivo/vitro. Comparing the k_{cat}/K_m values of carbapenems, the carbapenemase activity of NDM-5 was similar to NDM-24, but higher than NDM-1. A recent study showed that an increase of the catalytic efficiency (k_{cat}/K_m) for meropenem has been ascertained in NDM-5 (V88L and M154L). In NDM-4, which contains only M154L, no significant change has been observed, suggesting that V88L might play a role in enhancing the NDM enzymes activity rather than M154L. Moreover, an increase of the carbapenemase activity was also observed in the evolutionary NDM variants, such as NDM-17 (V88L, M154L, and E170K) and NDM-20 (V88L, M154L, and R270H) [10,15,16].

Table 2. Kinetic parameters of NDM-1, NDM-5, and NDM-24 toward β -lactams *a*.

Kinetic Parameters	Enzyme	β -Lactams ^b						
		AMP	PEN	TAG	FEP	MEM	IPM	ETP
$K_m(\mu\text{M})$	NDM-24	638.79 \pm 23.86	331.30 \pm 29.43	173.85 \pm 9.73	318.93 \pm 10.86	266.24 \pm 27.03	338.20 \pm 24.23	125.23 \pm 19.08
	NDM-1	1249.98 \pm 210.94	224.57 \pm 13.57	213.90 \pm 11.01	173.55 \pm 19.46	284.24 \pm 7.87	234.83 \pm 7.44	105.54 \pm 3.09
	NDM-5	825.00 \pm 0.29	315.21 \pm 46.68	76.45 \pm 4.76	179.64 \pm 12.19	275.16 \pm 36.87	292.97 \pm 13.76	82.18 \pm 3.86
$k_{\text{cat}} (\text{s}^{-1})$	NDM-24	259.94 \pm 23.52	179.10 \pm 8.17	43.13 \pm 1.06	22.98 \pm 0.34	151.75 \pm 6.69	173.16 \pm 8.83	110.31 \pm 7.62
	NDM-1	254.34 \pm 28.96	79.28 \pm 1.96	26.73 \pm 0.71	8.42 \pm 0.63	75.18 \pm 3.44	79.81 \pm 5.15	62.89 \pm 1.15
	NDM-5	346.13 \pm 31.30	214.13 \pm 12.11	26.96 \pm 0.75	13.05 \pm 0.24	142.48 \pm 17.91	149.63 \pm 2.02	83.18 \pm 1.67
$k_{\text{cat}}/K_m (\mu\text{M}^{-1} \text{s}^{-1})$	NDM-24	0.41	0.54	0.25	0.072	0.57	0.51	0.88
	NDM-1	0.20	0.35	0.13	0.046	0.26	0.34	0.60
	NDM-5	0.40	0.68	0.35	0.073	0.52	0.51	1.01
$k_{\text{cat}}/K_m (\mu\text{M}^{-1} \text{s}^{-1})$ ratio for:	NDM-24/NDM-1	2.00	1.53	1.98	1.49	2.16	1.51	1.46
	NDM-5/NDM-24	1.03	1.26	1.42	1.01	0.91	1.00	1.15
	NDM-5/NDM-1	2.07	1.92	2.82	1.50	1.96	1.50	1.68

^a The proteins were initially purified with a His-tag, which was removed after purification. Each kinetic value is the mean of three different measurements; the error was below 5%. ^b β -lactams: AMP, ampicillin; TAG, ceftazidime; PEN, penicillin G; FEP, cefepime; IPM, imipenem; MEM, meropenem; ETP, ertapenem.

2.4. Thermal Stability

As previously reported, mutations in the NDM variants can affect the enzymes stability, resulting in changing the persistence lifetime in the bacterial host, and consequent antibiotics resistance [25]. For determining whether the V88L substitution influences the NDM-24 stability property, circular dichroism CD was used to assay the protein stability by recording signal changes. NDM-5 was used as reference to analyze the effect of M154L. Compared with NDM-1 and NDM-5, NDM-24 (59.41 ± 0.06 °C) possessed the lowest melting temperature (Figure 2). Notably, the V88L destabilized effect was compensated by M154L in NDM-5 with a remarkable higher thermal temperature than NDM-24 (69.13 ± 3.6 °C compared to 59.41 ± 0.06 °C). Moreover, NDM-5 showed a higher stability than NDM-1 suggesting the destabilized role of M154L. This was in agreement with a previous document that the M154L mutation would be a turning point for the NDM variants, in which combining M154L with additional substitutions benefit for the NDM enzymes exhibiting increased thermostability [10]. In the NDM-24 group there are four variants (NDM-5, -17, -20, and -21) in which the combination of the V88L and M154L substitutions takes favorable results in terms of the stability and environmental selection.

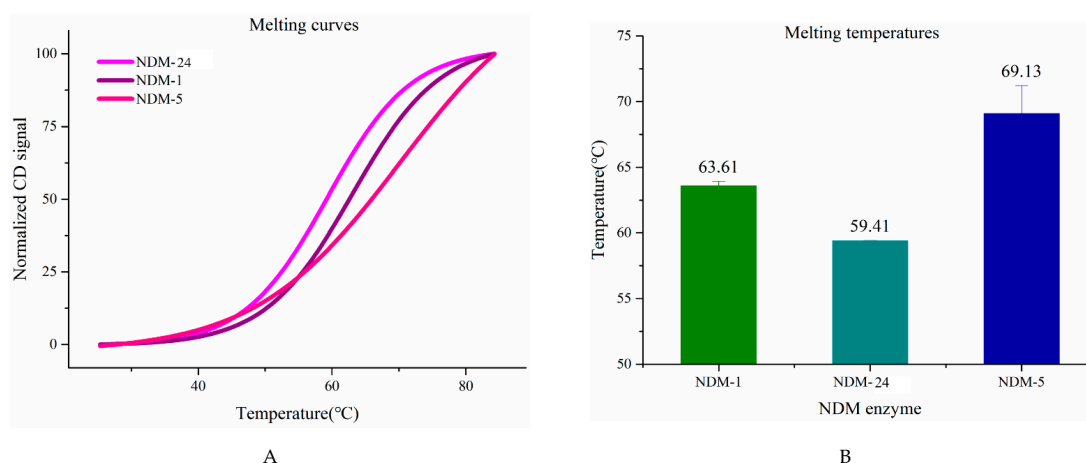


Figure 2. (A) Thermal stability melting curves. (B) Melting temperatures of the NDM enzymes as determined by the circular dichroism analysis: NDM-1, 63.61 ± 0.57 °C; NDM-V88L, 59.41 ± 0.06 °C; and NDM-5, 69.13 ± 3.6 °C. Data are the means of triplicate experiments, with error bars showing the standard deviation (\pm SD).

2.5. Structure Analysis

Previous reports indicated that mutations in the NDM influence the α -helical, β -sheets content, and loop flexibility [26]. For example, the Q123A substitution in NDM-1 leads to a decrease of the α -helical content [27]. To know if the V88L substitution could modify the NDM-24 structure, a secondary structure was determined by the Far-UV CD spectrum. All NDM variants CD spectrum data were fitted and shown in Figure 3. The spectrum signals were superimposable at most wavelengths, and showed characteristics of $\alpha\beta/\beta\alpha$ fold, a typical and conservative protein structure in MBLs [28]. The presence of positive bands at 192 nm and two negative peaks at 208 nm, a minimum peak, and 220 nm, suggesting the dominance of the β -sheets and α -helical content. The major differences were observed in the nearby 192 nm, symbolizing α -helical peak, and 208–220 nm, a α -helical and β -sheets bonds. Overall, the α -helical content was found ranging between 13%–20% in NDM-1, NDM-5, and NDM-24 (Table 3), in agreement with previous reports and the content of the β -sheet was high around 30% [27]. Compared to NDM-1, NDM-24 possesses a higher α -helical content and lower β -sheet content, suggesting that V88L was responsible for the secondary structure content changes of NDM-24. Furthermore, the secondary predicted result (Figure S3) confirmed that the V88L substitution occurred in the β -strand terminal, which may be prematurely terminated, leading to a decrease in the β -sheet content. Kumar et al. claimed that 152A, located in the β -strand, drastically influenced the NDM-5

activity and protein thermolability, by reducing the β -sheet content [26]. Our analysis demonstrates that the emergence of M154L (in NDM-5) caused the α -helical to decrease and the β -sheet to increase relative to NDM-24, while the α -helical and β -sheet content of NDM-5 were between NDM-1 and NDM-24. In addition, the 3D model of NDM-24 (Figure 4) was generated by using NDM-1 (PDB accession: 5N0H, 4RBS, 4HKY, and 4EYL) and NDM-5 (PDB accession: 6MGY, and 4TZE) as a template. Although the residue 88L is away from the active site groove and far to the active loops (Loop 3 and Loop 10), differences in the structure content, stability, and enzyme activity were ascertained. Several studies confirmed that non-activity sites substitution can influence the NDM catalytic efficiency [29], and our results about the V88L substitution support this theory.

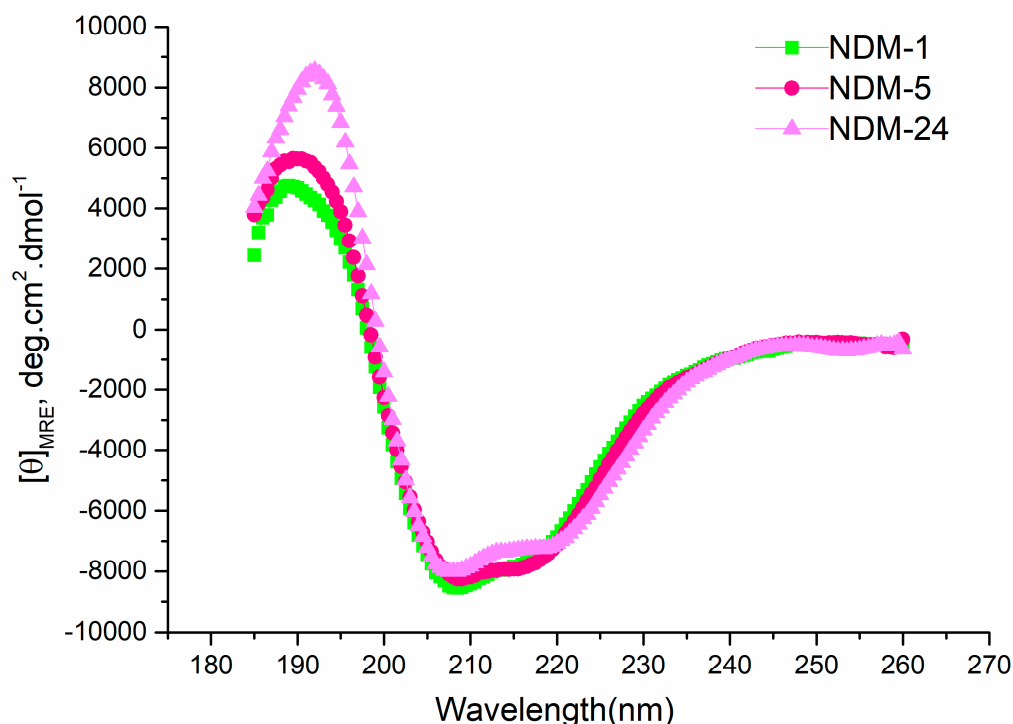


Figure 3. Normalized circular dichroism (CD) spectra of the NDM enzymes tested. MRE: Mean residue ellipticity.

Table 3. Proportions of various secondary structural elements in the NDM-1, NDM-5, and NDM-24 enzymes.

Program Algorithms ^a	Structural Elements ^b	SMP50(9) ^c			SP37(3) ^c			SP29(1) ^c		
		NDM-1	NDM-5	NDM-24	NDM-1	NDM-5	NDM-24	NDM-1	NDM-5	NDM-24
SELCON3	H(r)	0.070	0.078	0.092	0.062	0.074	0.092	0.059	0.079	0.087
	H(d)	0.085	0.088	0.089	0.081	0.088	0.089	0.078	0.087	0.086
	S(r)	0.215	0.199	0.195	0.228	0.214	0.195	0.231	0.191	0.196
	S(d)	0.115	0.109	0.108	0.117	0.113	0.108	0.118	0.107	0.108
	Trn	0.214	0.211	0.194	0.218	0.214	0.194	0.226	0.214	0.215
	Unrd	0.284	0.287	0.261	0.282	0.279	0.261	0.287	0.292	0.285
	H(r)+H(d)	0.155	0.166	0.181	0.143	0.162	0.181	0.137	0.166	0.173
	S(r)+S(d)	0.33	0.308	0.303	0.345	0.327	0.303	0.349	0.298	0.304
CONTINLL	H(r)	0.054	0.075	0.091	0.046	0.079	0.097	0.071	0.078	0.093
	H(d)	0.079	0.092	0.101	0.089	0.095	0.103	0.092	0.096	0.100
	S(r)	0.217	0.208	0.187	0.202	0.205	0.182	0.197	0.197	0.183
	S(d)	0.114	0.113	0.108	0.112	0.111	0.107	0.113	0.111	0.107
	Trn	0.233	0.220	0.220	0.248	0.216	0.216	0.231	0.222	0.225
	Unrd	0.303	0.292	0.293	0.304	0.293	0.294	0.297	0.297	0.292
	H(r)+H(d)	0.133	0.167	0.192	0.135	0.174	0.200	0.163	0.174	0.193
	S(r)+S(d)	0.331	0.321	0.295	0.314	0.316	0.289	0.310	0.308	0.290

^a The CDPro program package was used to analyse the data using two algorithms: CONTINLL and SELCON3.

^b H(r), regular α -helix; H(d), distorted α -helix; S(r), regular β -strand; S(d), distorted β -strand; Trn, turns; Unrd, unordered. ^c The reference protein sets (IBasis sets) were adopted.

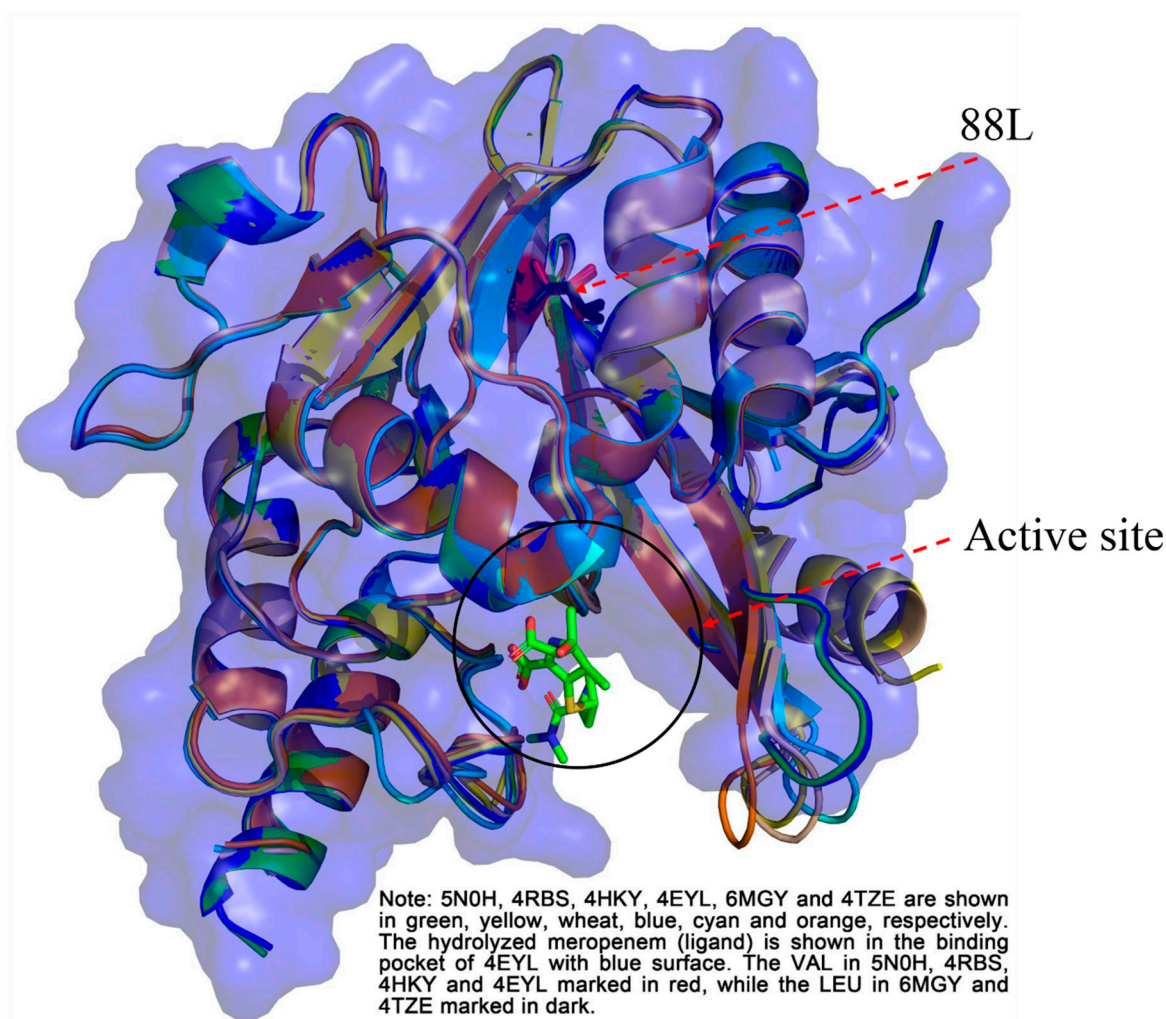


Figure 4. Cartoon model of NDM-24. To acquire a credible model, the 6 NDM crystal structure (NDM-1(5N0H, 4RBS, 4HKY, and 4EYL) and NDM-5(6MGY, and 4TZE)) were adopted. The residue 88L and active pocket were labelled.

3. Material and Methods

3.1. Site-Directed Mutagenesis, Cloning and Expression of NDM Variants

The *bla*_{NDM-1} and *bla*_{NDM-5} encoding genes were obtained from clinical *Escherichia coli* strains as previously described [15,16]. Site-directed mutagenesis was performed to generate *bla*_{NDM-24} using the pHSG398/NDM-1 plasmid as template and primers listed in Table S1, as previously described [30].

First, the *bla*_{NDM}-genes were cloned into a pHSG398 vector (TaKaRa Bio, Dalian, China) using the *Bam*HI and *Xho*I restriction sites. In a second PCR experiment, the *bla*_{NDM} variants were amplified without a signal peptide introducing the Tobacco Etch Virus (TEV) at the N-terminal sequence. In order to obtain enzymes overexpression, the amplicons were inserted into a pET-28a(+) plasmid. The *E. coli* DH5 α competent cells were used as a non-expression host. *E. coli* BL21(DE3) was used for enzymes overexpression. The authenticity of recombinant plasmids was verified by PCR and sequencing was with Sanger.

3.2. Antimicrobial Susceptibility Tests

The phenotypic profile has been characterized by a microdilution method using a bacterial inoculum of 5×10^5 CFU/ml according to the Clinical Laboratory and Standards Institute [31,32]. *E. coli* ATCC25922 was used as a negative control.

3.3. Production and Purification of NDM-1, NDM-5, and NDM-24

NDM-1, NDM-5, and NDM-24 were extracted from 0.5 L of culture of *E. coli* BL21(DE3)/pETNDM-1, *E. coli* BL21 (DE3) /pETNDM-5, and *E. coli* BL21 (DE3)/pETNDM-24, respectively. The cultures were grown at 37 °C to achieve an A_{600} of 0.5 L, and 0.4 mM of IPTG was added. After addition of the IPTG, the cultures were incubated at 20 °C for 16 h, under aerobic conditions. Thereafter, a cell supernatant containing the soluble NDM protein was obtained from the lytic bacteria by centrifuging at 10⁴ rpm. Proteins purification followed the manufacturer's instructions (Qiagen, Hilden, Germany) by using the Ni-nitrilotriacetic acid (NTA) agarose. The turbo tobacco etch virus (TEV) protease (Accelagen, San Diego, CA, USA) was used to gain the untagged protein without the His tags. The SDS-PAGE was performed to estimate the NDM purity enzymes. The protein concentration was determined using a BCA Protein Quantification Kit (Vazyme Biotech Co., Ltd, Nanjing, China). The β -lactamase activity was monitored at each purification step using the colour change of nitrocefin 1 mg/mL, a chromogenic cephalosporin, according to the previous report [20].

3.4. Determination of Kinetic Parameters

Steady-state kinetic experiments were performed following the hydrolysis of each substrate at 25 °C in a 50 mM phosphate buffer, pH 7.0 in the presence of 20 μ M Zn SO₄. The data were collected with a SpectraMax M5 multi-detection microplate reader (Molecular Devices, Sunnyvale, CA, USA) as previously described [33]. Kinetic parameters were determined under initial-rate conditions using the GraphPad Prism[®] version 5.01 (San Diego, CA, USA) to generate the Michaelis-Menten curves, or by analysing the complete hydrolysis time courses [34,35]. Each kinetic value is the mean of the results of three different measurements. The error was below 5%. NDM-5 was used as a reference to normalize.

3.5. Circular Dichroism and Structure Analysis

The circular dichroism (CD) spectra (185 to 260 nm) were determined with a Chirascan Plus CD spectrophotometer (Applied Photophysics Ltd, Leatherhead, UK) equipped with a Peltier temperature-controlled cell holder, at 25 °C using a 1-mm pathlength cuvette and the Savitzky-Golay filter was explored to the baseline-correct spectra data. Protein concentrations were diluted to 0.05–0.2 mg/mL with a 5 mM sodium phosphate buffer pH 7.0 [36]. 207 nm spectrum data was used as the baseline to normalize and calibrate data for eliminating minor errors due to different concentrations [37]. The analysis was performed using the CONTINLL and SELCON3 algorithms with reference data sets three and nine, respectively [38]. The super-secondary (tertiary) structures of the proteins were analysed by the CDPPro software package, which is available at the CDPPro website: <https://sites.bmb.colostate.edu/sreeram/CDPro/> [38,39]. To assay the location of the V88L substitution and analyse its effect on the structure, the pharmacophore modeling and screening software program Discovery Studio (version 2018) was employed to generate a three-dimensional (3D) interconnected model of NDM-24 using NDM-1 and NDM-5 as a template, in which reliable data of the crystal structure were collected from the PDB database.

3.6. Thermal Stability Testing

The melting temperature (T_m) was used to show the protein stability. The determination of T_m was performed by recording the CD signal change at 222 nm. Data were collected at a ramp of 1 °C /min with a temperature range from 20–90 °C. The two-state model using nonlinear regression (Boltzmann) in the OriginPro 9.1.64 (OriginLab, Northampton, MA, USA) was applied to analyse the data. When 50% of the protein melts, the temperature is defined as the T_m , representing thermal stability.

4. Conclusions

Our study explored the NDM-24 biological function and probed the V88L substitution role on the structure, enzyme activity, and stability. In brief, this non-active site change enhances the

enzyme activity by increasing the turnover rate, related with an indirect effect on conformation. However, the loss cost caused by V88L significantly decreased the protein stability, and would shorten the persistence lifetime in the cell, so that the resistance to antibiotics hardly exhibits an outstanding elevation for the NDM-24-producing transformants. Meanwhile, alterations in the secondary content, such as lowering the β -sheet, have an interesting role in the NDM instability, being relevant to the V88L substitution occurring in the β -strand. According to previous data, the V88L/M154L combination appears to be favorable in the NDM evolution under an environmental pressure selection [14]. Further analysis about the significance of non-active-site residues will help in the comprehension of the resistance mechanism and broaden insight in the development of inhibitors, such as potential antibiotics candidate by reducing the protein stability lifetime.

Supplementary Materials: The following are available online at <http://www.mdpi.com/2073-4344/9/9/744/s1>. Figure S1: SDS-PAGE of NDM-24. Lane 1: NDM-24 containing His Tags, Figure S2: Molecular mass spectrometry of NDM-24 estimated by MALDI-TOF, Figure S3: Predicted secondary structure of NDM-24, Lane 2: NDM was cleaved by using Turbo tobacco etch virus (TEV) protease to remove His Tags (Accelagen, San Diego, CA, USA): tagged protein (2a) and untagged protein (2b); Lane 3: untagged protein; Lane M: Marker, Table S1. Oligonucleotides used in this study.

Author Contributions: J.S. designed the study. Z.L., D.L., and W.L. collected the data. Z.L., Y.W., and D.L. analyzed and interpreted the data. Z.L., A.P., D.L., Y.W., and J.S. wrote the report. All authors revised, reviewed and approved the final report.

Funding: The study was supported by grants from the National Key Research and Development Program of China (2018YFD0500300), and the National Natural Science Foundation of China (81861138051 and 81661138002).

Conflicts of Interest: The author declares no conflict of interest.

References

1. Palzkill, T. Metallo-beta-lactamase structure and function. *Ann. N. Y. Acad. Sci.* **2013**, *1277*, 91–104. [[CrossRef](#)] [[PubMed](#)]
2. Garau, G.; García-Sáez, I.; Bebrone, C.; Anne, C.; Mercuri, P.; Galleni, M.; Frère, J.M.; Dideberg, O. Update of the standard numbering scheme for class B beta-lactamases. *Antimicrob. Agents Chemother.* **2004**, *48*, 2347–2349. [[CrossRef](#)] [[PubMed](#)]
3. Yong, D.; Toleman, M.A.; Giske, C.G.; Cho, H.S.; Sundman, K.; Lee, K.; Walsh, T.R. Characterization of a New Metallo- β -Lactamase Gene, blaNDM-1, and a Novel Erythromycin Esterase Gene Carried on a Unique Genetic Structure in *Klebsiella pneumoniae* Sequence Type 14 from India. *Antimicrob. Agents Chemother.* **2009**, *53*, 5046–5054. [[CrossRef](#)] [[PubMed](#)]
4. Bonnin, R.A.; Poirel, L.; Carattoli, A.; Nordmann, P. Characterization of an IncFII Plasmid Encoding NDM-1 from *Escherichia coli* ST131. *PLoS ONE* **2012**, *7*, 34752. [[CrossRef](#)] [[PubMed](#)]
5. Dolejska, M.; Villa, L.; Poirel, L.; Nordmann, P.; Carattoli, A. Complete sequencing of an IncHI1 plasmid encoding the carbapenemase NDM-1, the ArmA 16S RNA methylase and a resistance-nodulation-cell division/multidrug efflux pump. *J. Antimicrob. Chemother.* **2013**, *68*, 34–39. [[CrossRef](#)] [[PubMed](#)]
6. King, D.; Strynadka, N. Crystal structure of New Delhi metallo-beta-lactamase reveals molecular basis for antibiotic resistance. *Protein Sci.* **2011**, *20*, 1484–1491. [[CrossRef](#)] [[PubMed](#)]
7. Gonzalez, L.J.; Bahr, G.; Nakashige, T.G.; Nolan, E.M.; Bonomo, R.A.; Vila, A.J. Membrane anchoring stabilizes and favors secretion of New Delhi metallo-beta-lactamase. *Nat. Chem. Biol.* **2016**, *12*, 516–522. [[CrossRef](#)] [[PubMed](#)]
8. Gonzalez, L.J.; Bahr, G.; Vila, A.J. Lipidated beta-lactamases: From bench to bedside. *Future Microbiol.* **2016**, *11*, 1495–1498. [[CrossRef](#)]
9. Khan, A.U.; Maryam, L.; Zarrilli, R. Structure, genetics and worldwide spread of New Delhi metallo-beta-lactamase (NDM): A threat to public health. *BMC Microbiol.* **2017**, *17*, 101. [[CrossRef](#)]
10. Cheng, Z.; Thomas, P.W.; Ju, L.; Bergstrom, A.; Mason, K.; Clayton, D.; Miller, C.; Bethel, C.R.; Vanpelt, J.; Tierney, D.L.; et al. Evolution of New Delhi metallo- β -lactamase (NDM) in the clinic: Effects of NDM mutations on stability, zinc affinity, and mono-zinc activity. *J. Biol. Chem.* **2018**, *293*, 12606–12618. [[CrossRef](#)]

11. Zhang, H.O.; Hau, Q. Crystal structure of NDM-1 reveals a common β -lactam hydrolysis mechanism. *FASEB J.* **2011**, *25*, 2574–2582. [[CrossRef](#)] [[PubMed](#)]
12. Kim, Y.; Cunningham, M.A.; Mire, J.; Tesar, C.; Sacchettini, J.; Joachimiak, A. NDM-1, the ultimate promiscuous enzyme: Substrate recognition and catalytic mechanism. *FASEB J.* **2013**, *27*, 1917–1927. [[CrossRef](#)] [[PubMed](#)]
13. Liu, L.; Feng, Y.; McNally, A.; Zong, Z. bla NDM-21, a new variant of blaNDM in an Escherichia coli clinical isolate carrying blaCTX-M-55 and rmtB. *J. Antimicrob. Chemother.* **2018**, *73*, 2336–2339. [[CrossRef](#)] [[PubMed](#)]
14. Bahr, G.; Vitor-Horen, L.; Bethel, C.R.; Bonomo, R.A.; González, L.J.; Vila, A.J. Clinical evolution of New Delhi Metallo- β -lactamase (NDM) optimizes resistance under Zn(II) deprivation. *Antimicrob. Agents Chemother.* **2018**, *62*, 1817–1849. [[CrossRef](#)] [[PubMed](#)]
15. Liu, Z.; Li, J.; Wang, X.; Liu, D.; Ke, Y.; Wang, Y.; Shen, J. Novel Variant of New Delhi Metallo- β -lactamase, NDM-20, in Escherichia coli. *Front. Microbiol.* **2018**, *9*, 248. [[CrossRef](#)] [[PubMed](#)]
16. Liu, Z.; Wang, Y.; Walsh, T.R.; Liu, D.; Shen, Z.; Zhang, R.; Yin, W.; Yao, H.; Li, J.; Shen, J. Plasmid-mediated novel bla_{NDM-17} gene encoding a carbapenemase with enhanced activity in a ST48 Escherichia coli strain. *Antimicrob. Agents Chemother.* **2017**, *61*, 2216–2233. [[CrossRef](#)] [[PubMed](#)]
17. Nordmann, P.; Boulanger, A.E.; Poirel, L. NDM-4 Metallo- β -Lactamase with Increased Carbapenemase Activity from Escherichia coli. *Antimicrob. Agents Chemother.* **2012**, *56*, 2184–2186. [[CrossRef](#)]
18. Zou, D.; Huang, Y.; Zhao, X.; Liu, W.; Dong, D.; Li, H.; Wang, X.; Huang, S.; Wei, X.; Yan, X.; et al. A Novel New Delhi Metallo- β -Lactamase Variant, NDM-14, Isolated in a Chinese Hospital Possesses Increased Enzymatic Activity against Carbapenems. *Antimicrob. Agents Chemother.* **2015**, *59*, 2450–2453. [[CrossRef](#)]
19. Tada, T.; Miyoshi-Akiyama, T.; Dahal, R.K.; Sah, M.K.; Ohara, H.; Kirikae, T.; Pokhrel, B.M. NDM-8 Metallo- β -Lactamase in a Multidrug-Resistant Escherichia coli Strain Isolated in Nepal. *Antimicrob. Agents Chemother.* **2013**, *57*, 2394–2396. [[CrossRef](#)]
20. Tada, T.; Shrestha, B.; Miyoshi-Akiyama, T.; Shimada, K.; Ohara, H.; Kirikae, T.; Pokhrel, B.M. NDM-12, a Novel New Delhi Metallo- β -Lactamase Variant from a Carbapenem-Resistant Escherichia coli Clinical Isolate in Nepal. *Antimicrob. Agents Chemother.* **2014**, *58*, 6302–6305. [[CrossRef](#)]
21. Ines, S.; Emma, K.; Rudolf, R.; Rumyana, M.; Anne Marie, Q.; Adolf, B. VIM-15 and VIM-16, two new VIM-2-like metallo-beta-lactamases in Pseudomonas aeruginosa isolates from Bulgaria and Germany. *Antimicrob. Agents Chemother.* **2008**, *52*, 2977.
22. Patricia, M.; Tomatis, P.E.; Mussi, M.A.; Fernando, P.; Viale, A.M.; Limansky, A.S.; Vila, A.J. Biochemical characterization of metallo-beta-lactamase VIM-11 from a Pseudomonas aeruginosa clinical strain. *Antimicrob. Agents Chemother.* **2008**, *52*, 2250.
23. Jose-Manuel, R.M.; Patrice, N.; Nicolas, F.; Laurent, P. VIM-19, a metallo-beta-lactamase with increased carbapenemase activity from Escherichia coli and Klebsiella pneumoniae. *Antimicrob. Agents Chemother.* **2010**, *54*, 471–476.
24. Pierre, B.; Carine, B.; Te-Din, H.; Warda, B.; Yves, D.; Ariane, D.; Kurt, H.; Youri, G. Detection and characterization of VIM-31, a new variant of VIM-2 with Tyr224His and His252Arg mutations, in a clinical isolate of Enterobacter cloacae. *Antimicrob. Agents Chemother.* **2012**, *56*, 3283.
25. Corbin, B.D.; Seeley, E.H.; Raab, A.; Feldmann, J.; Miller, M.R.; Torres, V.J.; Anderson, K.L.; Dattilo, B.M.; Dunman, P.M.; Gerads, R.; et al. Metal Chelation and Inhibition of Bacterial Growth in Tissue Abscesses. *Science* **2008**, *319*, 962–965. [[CrossRef](#)] [[PubMed](#)]
26. Kumar, G.; Issa, B.; Kar, D.; Biswal, S.; Ghosh, A.S. E152A substitution drastically affects NDM-5 activity. *FEMS Microbiol. Lett.* **2017**, *364*. [[CrossRef](#)] [[PubMed](#)]
27. Ali, A.; Azam, M.W.; Khan, A.U. Non-active site mutation (Q123A) in New Delhi metallo- β -lactamase (NDM-1) enhanced its enzyme activity. *Int. J. Biol. Macromol.* **2018**, *112*, 1272–1277. [[CrossRef](#)] [[PubMed](#)]
28. Carfi, A.; Pares, S.; Duée, E.; Galleni, M.; Duez, C.; Frère, J.M.; Dideberg, O. The 3-D structure of a zinc metallo-beta-lactamase from Bacillus cereus reveals a new type of protein fold. *EMBO J.* **1995**, *14*, 4914–4921. [[CrossRef](#)] [[PubMed](#)]
29. Piccirilli, A.; Brisdelli, F.; Aschi, M.; Celenza, G.; Amicosante, G.; Perilli, M. Kinetic Profile and Molecular Dynamic Studies Show that Y229W Substitution in an NDM-1/L209F Variant Restores the Hydrolytic Activity of the Enzyme toward Penicillins, Cephalosporins, and Carbapenems. *Antimicrob. Agents Chemother.* **2019**, *63*, e02270-18. [[CrossRef](#)]
30. Meini, M.-R.; Tomatis, P.E.; Weinreich, D.M.; Vila, A.J. Quantitative Description of a Protein Fitness Landscape Based on Molecular Features. *Mol. Biol. Evol.* **2015**, *32*, 1774–1787. [[CrossRef](#)]

31. Clinical and Laboratory Standards Institute. *Methods for Dilution Antimicrobial Susceptibility Tests for Bacteria that Grow Aerobically: Approved Standard*, 11th ed.; CLSI document M07; Clinical and Laboratory Standards Institute: Wayne, PA, USA, 2018.
32. Clinical and Laboratory Standards Institute. *Performance Standards for Antimicrobial Susceptibility Testing*, 28th ed.; CLSI document M100; Clinical and Laboratory Standards Institute: Wayne, PA, USA, 2018.
33. Crowder, M.W.; Walsh, T.R.; Banovic, L.; Pettit, M.; Spencer, J. Overexpression, purification, and characterization of the cloned metallo-beta-lactamase L1 from *Stenotrophomonas maltophilia*. *Antimicrob. Agents Chemother.* **1998**, *42*, 921. [[CrossRef](#)] [[PubMed](#)]
34. De Meester, F.; Joris, B.; Reckinger, G. Automated analysis of enzyme inactivation phenomena. Application to β -lactamases and DD-peptidases. *Biochem. Pharmacol.* **1987**, *36*, 2393–2403. [[CrossRef](#)]
35. Segel, I.H. *Biochemical Calculations*, 2nd ed.; John Wiley & Sons: New York, NY, USA, 1976; pp. 236–241.
36. Liu, Z.; Zhang, R.; Li, W.; Yang, L.; Liu, D.; Wang, S.; Shen, J.; Wang, Y. Amino acid changes at the VIM-48 C-terminus result in increased carbapenem resistance, enzyme activity and protein stability. *J. Antimicrob. Chemother.* **2018**, *74*, 885–893. [[CrossRef](#)] [[PubMed](#)]
37. Raussens, V.; Ruysschaert, J.-M.; Goormaghtigh, E. Protein concentration is not an absolute prerequisite for the determination of secondary structure from circular dichroism spectra: A new scaling method. *Anal. Biochem.* **2003**, *319*, 114–121. [[CrossRef](#)]
38. Sreerama, N.; Venyaminov, S.Y.; Woody, R.W. Estimation of the number of α -helical and β -strand segments in proteins using circular dichroism spectroscopy. *Protein Sci.* **1999**, *8*, 370–380. [[CrossRef](#)] [[PubMed](#)]
39. Sreerama, N.; Venyaminov, S.Y.; Woody, R.W. Analysis of Protein Circular Dichroism Spectra Based on the Tertiary Structure Classification. *Anal. Biochem.* **2001**, *299*, 271–274. [[CrossRef](#)] [[PubMed](#)]



© 2019 by the authors. Licensee MDPI, Basel, Switzerland. This article is an open access article distributed under the terms and conditions of the Creative Commons Attribution (CC BY) license (<http://creativecommons.org/licenses/by/4.0/>).